Catalysis Science & Technology

Accepted Manuscript

ROYAL SOCIETY OF CHEMISTRY

www.rsc.org/catalysis

Catalysis Science &Technology

PAPER

Ligand Effect of SnO_2 on Pt-Ru Catalyst and Relation between Bond Strength and CO Tolerance

Received 00th January 20xx,
Accepted 00th January 20xx

DOI: 10.1039/x0xx00000x

www.rsc.org/

Tatsuya Takeguchi[a]*, Akane Kunifuji[b], Napan Narischat[ab], Mikio Ito[c], Hidenori Noguchi[d], Kohei Uosaki[d] and Shin R. Mukai[b]

Pt-Ru/SnO_2/C catalysts were prepared by rapid quenching method. The structure and morphology of Pt-Ru particles of Pt-Ru/SnO_2/C are controlled to obtain the same Pt-Ru particle as commercial Pt-Ru catalyst. Pt-Ru/SnO_2/C and commercial Pt-Ru catalyst were characterized by x-ray diffraction and scanning transmission electron microscopy. Electrochemical activities were evaluated by CO stripping voltammetry, a single cell test, in situ infrared reflection–absorption spectroscopy (IRRAS), and surface-enhanced infrared absorption spectroscopy (SEIRAS). Pt-Ru/SnO_2/C catalyst showed the same structure, morphology, and catalytic activity for hydrogen oxidation reaction (HOR) in the absence of CO as Pt-Ru/C catalyst. Both of activity of electrochemical CO oxidation and the Pt-CO bond strength were quantitatively evaluated. The addition of SnO_2 decreasing Pt-CO bond strength with maintaining HOR activity to enhanced CO tolerance.

Introduction

The residential cogeneration systems with polymer electrolyte fuel cell (PEFC) have been attracting great interest as one of the promising power sources, since fuel cell systems are expected to contribute to the reduction of CO_2 emission. Generally, reformate H_2 gas, produced from city gas which is mainly composed of CH_4, is used as fuel for PEFC. Because CO is contained in reformate H_2, the anode catalyst is deactivated by the adsorption of CO. The Pt-Ru/C catalyst has been recognized as the most active catalyst, and the bifunctional mechanism[1, 2] is usually considered to contribute to the CO tolerance. On the other hand, it was reported that various Pt alloy catalyst, such as Pt-Sn, Pt-Fe, and Pt-Co showed high CO tolerance[3-7]. Mukerjee et al. reported that Pt-Mo alloy catalyst (Pt:Mo=5:1) showed high performance[8]. For metal oxide-modified systems, it was reported that the addition of SnO_2, TiO_2, and NbO_x enhanced CO tolerance[9-11]. Ioroi et al. reported that Pt/MO_x/C system showed higher CO tolerance than Pt-Ru catalysts[12]. The unoccupied orbital of transition metal suppress the back-donation of 5d electron Pt to CO, resulting in the week bond strength of Pt-CO (ligand effect)[13]. Not only Pt-alloys but also supports can affect Pt electronic structure. Nakamura et al. reported the evidence that support has an interaction with Pt, resulting in a modification of Pt electronic structure and lowering adsorption energy of CO [14-17]. The PtMo/C[8, 18-20] and $PtSnO_x$[21-24] catalysts are investigated for H_2/CO electrochemical oxidation, and the promotional effect of Mo in the PtMo/C catalyst and SnO_x in the $PtSnO_x$ catalysts on CO tolerance were observed. Compared with that on the Pt-Ru/C catalyst, a lower onset potentials of electrochemical CO oxidation[4, 25, 26] are obtained on the PtMo/C and $PtSnO_x$ catalysts. Electrochemical oxidation of CO does not significantly contribute to CO tolerance. Weakening of Pt-CO bond strength caused by ligand effect contributes to CO tolerance; however, it is hard to evaluate Pt-CO bond strength quantitatively in situ. Weakening of Pt-CO bond strength often decrease HOR activity[27-29] in membrane electrode assembly (MEA), and CO tolerance was not improved in these cases.

In this study, we aimed quantitative evaluation of Pt-CO bond strength, electrochemical CO oxidation, and HOR activity in MEA. Pt-Ru/SnO_2/C catalysts were prepared by rapid quenching method[30, 31]. The structure and morphology of Pt-Ru particle of Pt-Ru/SnO_2/C are controlled to prepare the same Pt-Ru particle. The activities for electrochemical CO oxidation were evaluated by CO stripping voltammetry and in situ infrared reflection–absorption spectroscopy (IRRAS)[32-34]. The Pt-CO bond strengths were evaluated by SEIRAS[5, 35]. The HOR activities were evaluated by single cell in the absence/presence of CO.

Experimental

Catalyst synthetic procedures Materials and methods

[a] Department of Chemistry and Biological Sciences, Faculty of Science and Engineering, Iwate University, Iwate 020-8551, Japan.
[b] Graduate School of Engineering, Hokkaido University, Hokkaido 060-8628, Japan.
[c] Department of Chemical Science and Engineering, National Institute of Technology, Tokyo College 1220-2, Kunugida-machi, Hachioji, Tokyo 193-0997, Japan.
[d] International Center for Materials Nanoarchitectonics (MANA) and Global Research Center for Environment and Energy based on Nanomaterials Science (GREEN), National Institute for Materials Science, 1-1 Namiki, Tsukuba 305-0044, Japan.

$SnCl_2$ and ethylene glycol were mixed and stirred in a glass bottle at 190°C for 0.5 h to form SnO_2 colloid. After cooling to the room temperature, carbon black, E-type carbon from Tanaka Kikinzoku Kogyo K.K., was added to the mixed solution, which was stirred at 190°C overnight. SnO_2/C sample obtained were filtered and washed with hot distilled water. Then the samples were dried in 60 ml/min stream of N_2 at 80°C overnight to form 4 wt% SnO_2/C.

Second, 40 wt% Pt/SnO_2/C was prepared. SnO_2/C, a solution of $Pt(NO_2)_2(NH_2)_2$ (4.597 wt% as Pt) from Tanaka Kikinzoku Kogyo, ethanol, and distilled water were mixed at 95°C overnight. 40 wt% Pt/SnO_2/C catalyst obtained were filtered and washed with hot distilled water. Then the samples were dried in 60 ml/min stream of N_2 at 80°C overnight to form 40 wt% Pt/SnO_2/C.

Next, Pt-Ru/SnO_2/C catalysts of Pt:Ru = 2:3 were prepared. 40 wt% Pt/SnO_2/C, $RuCl_3{\cdot}nH_2O$, methanol, and distilled water were mixed and stirred in a glass bottle at 70°C. During this process, Ru was reduced by methanol and adhered to Pt/C. The molar ratio of Pt : Ru in the catalysts a were 2:3. After 12 h of stirring, the catalysts obtained were filtered and washed with hot distilled water. Then the catalysts were dried in 60 ml/min stream of N_2 at 80°C overnight.

Finally, the catalysts were treated with He for 0.5 h, H_2/Ar (5% H_2) for 1 h, followed by for He for 1 h at the room temperature. Then, catalysts were treated with He during rapid heating to 900°C within 10 min. The oven was turned off immediately when the temperature had reached 900°C to rapidly cool the catalyst. The temperature decreased from 900 to 500°C in 18 min and decreased from 500°C to room temperature in about 50 min, followed by reduction in H_2/Ar (5% H_2) for 2 h at 150°C. Commercial catalyst, Pt_2Ru_3/TKK TEC61E54 (Pt 29.6%, Ru 23.0%, Tanaka Kikinzoku Kogyo), was used as a reference.

Physical characterization

XRD patterns of the Pt-Ru/SnO_2/C catalysts were recorded with a powder x-ray diffractometer (RIGAKU, RINT 2000) using Cu K*a* radiation with a Ni filter. The tube current was 20 mA with a tube voltage of 40 kV. The 2θ angular regions between 10 and 85° were explored at a scan rate of 5°/min. The morphology of the Pt-Ru/SnO_2/C catalysts was investigated by using a STEM (Hitachi HD-2000) at 200 kV and 30 mA.

CO stripping voltammetry was carried out in a 250 mL three-electrode cell (HR200, Hokuto Denko Corp.) at 25°C. A commercial glassy carbon (GC) electrode (HR2-D1-GC-5, 5 mm in diameter, Hokuto Denko Corp.), a Pt-wire electrode (0.3 mm in diameter, Hokuto Denko Corp.) and a saturated calomel electrode (Hokuto Denko Corp.) were used as a working electrode, counter electrode, and reference electrode, respectively. The potential of the working electrode was controlled by an Iviumstat Electrochemical Interface System (Ivium Technologies B.V.). 6 mg of the catalyst was dispersed in a mixture of 2 mL water, 3 mL ethanol, and 50 µL Nafion solution (5 wt %, Aldrich) with ultrasonic stirring to form a homogeneous catalyst ink. The catalyst layer was prepared by dropping 10 µL of the catalyst ink (PtRu ≈ 6.4 µg) onto a GC disk electrode by a microsyringe and drying at room temperature. All potential values in this paper are referred to a reversible hydrogen electrode. Pure CO was supplied into the electrolyte solution (0.1 M $HClO_4$) for 20 min at a fixed potential of 0.05 V at 60°C and then high-purity (99.99%) Ar was bubbled for 30 min to remove the CO dissolved in the electrolyte solution. Current–potential cycles were obtained from 0.05 to 1.2 V at a scan rate of 10 mV/s.

In situ IRRAS measurements were carried out in a homemade PTFE cell with a CaF_2 optical window using a JASCO FT/IR-6100 spectrometer equipped with a TGS detector[21, 36]. A gold disk (10 mm in diameter) was used as an electrode substrate for IRRAS measurements. The catalyst layers were deposited on the gold electrode surface by the same method as described for the CO stripping voltammetry experiments. Adsorption of CO was conducted first by bubbling CO into the cell for 20 min under potential control at 0.0 V, and then high-purity Ar was bubbled for 35 min to remove the CO dissolved in the electrolyte solution. Then the electrode was pushed onto the CaF_2 prism window with the thin-layer geometry to reduce the IR absorption by aqueous solution. The in situ IR spectra were recorded with a scan rate of 0.25 mV/s, and 25 interferograms were co-added to each spectrum. The recorded spectrum at the potential, that adsorbed CO was completely oxidized, was used a reference spectrum of adsorbed CO. The spectrum recorded at 0.0 V was used as a reference spectrum of the production of CO_2.

The SEIRAS experiments were carried out using a vertical spectro-electrochemical cell in Kretschmann ATR configuration as shown in Fig. 1. The working electrode was an Au thin film prepared by electroless deposition onto the hemicylindrical Si prism (Pier optics)[37]. A thin gold foil was used for the electrical contact with the Au thin film. Pt wire and Ag/AgCl (sat. NaCl) were used as counter and reference electrodes, respectively. Electrode potential was controlled by a potentiostat (Hokuto Denko, HA-151B) and a function generator (Hokuto Denko, HB-111). 0.5 M H_2SO_4 solution was used as an electrolyte solution. After CO gas was introduced in to the spectro-electrochemical cell at -150 mV, CO remaining in the solution was removed by bubbling Ar gas through the electrolyte solution for 30 min. Consequently, CO should exist only on the Pt-Ru surface at the initial stage of the experiments. The spectra were collected with p-polarized light and the spectral resolution was 2 cm^{-1}. All the measurements were carried out at room temperature.

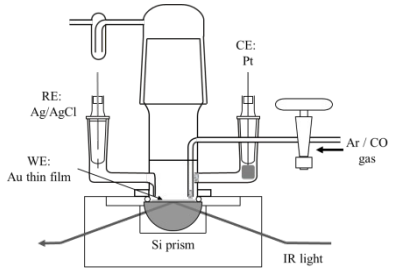

Fig. 1. Schematic diagram of surface-enhanced infrared absorption spectroscopy (SEIRAS) glass cell.

Fuel Cell Test

For preparation of MEA, carbon paper was used as the backing layers of the anode and cathode. Anode catalysts, Pt-Ru/C and Pt-Ru/SnO_2/C, and nafion solution were ultrasonically suspended in water. The carbon paper was painted with the catalyst ink. The loading of Pt-Ru in the anode catalyst layer was 0.5 mg cm^{-2}. In all cases, an identical cathode catalyst layer was prepared by the same procedure. A commercial Pt/C cathode catalyst (40 wt % Pt) was used instead of Pt-Ru/C catalysts, and the loadings of Pt in the cathode layer were 0.5 mg cm^{-2}. Finally, the anode and cathode (22 × 22 mm) were placed onto the two sides of a nafion NRE-212 membrane (Aldrich) and hot-pressed at 135°C and 4 MPa for 10 min to form the MEA. The MEA was assembled into a single cell with flow field plates made of graphite and copper end plates attached to a heater (FC05-01SP, ElectroChem, Inc.). The single cell was connected to fuel cell test equipment (Chino Corp.). Pure H_2 (or H_2/CO mixture) and O_2 were supplied at flow rates of 80 mL/min to the anode and cathode, respectively, at ambient pressure. During the measurement, a single cell was operated at 75°C, and the anode and cathode humidifiers were set at 75 and 70°C, respectively.

Results and discussion,

Powder x-ray diffractometer

XRD patterns of Pt-Ru/C and Pt-Ru/SnO_2/C catalysts are shown in Fig. 2. Both of the catalysts showed similar diffraction peaks. The broad peak at around 26° is assigned to C(002) plane as it can observed for both samples. The diffraction peak at around 40 and 69 are assigned to Pt (111) and (220) plane. If Ru and Pt with (Ru/Pt molar ratio of 1.5) make a merely complete alloy, peak at Pt (220) plane is expected to appear at 68.8°, based on the following equation[38, 39].

$a = a_0 - 0.124\ \chi_{Ru}$ (χ_{Ru}: Ru atomic fraction)

Both of Pt-Ru/C and Pt-Ru/SnO_2/C catalyst showed a Pt (220) plane peak at 68.8°, this indicates that alloying degrees of both Pt-Ru/C and Pt-Ru/SnO_2/C catalysts are identical and high enough. The possible SnO_2(110) peak is at 25°, which is interfered by C(002), then it cannot calculate the SnO_2 crystallite size.

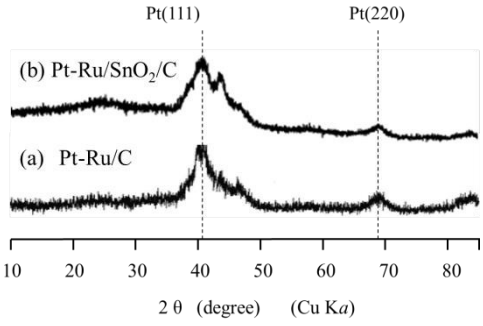

Fig. 2. XRD patterns of (a) Pt-Ru/C and (b) Pt-Ru/SnO_2/C.

STEM images

Fig. 3 shows STEM images of Pt-Ru/C and Pt-Ru/SnO_2/C catalysts. Both of the catalysts have similar morphologies with a uniform distribution on the carbon support and similar particle size distribution. Particle sizes of both catalysts ranging from 2 to 4 nm. These data suggested that the structure and morphology of Pt-Ru particle of Pt-Ru/SnO_2/C are the same as that of Pt-Ru/C. The SnO_2 cannot recognize by STEM images due to the low content as 1.84%.

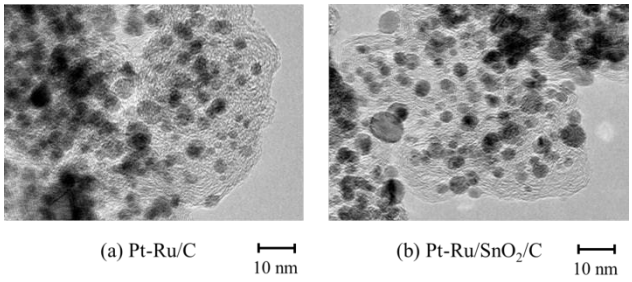

Fig. 3. STEM images of (a) Pt-Ru/C and (b) Pt-Ru/SnO_2/C.

CO stripping voltammetry

Fig. 4 shows the results of CO stripping voltammetry at 60°C for of both Pt-Ru/C and Pt-Ru/SnO_2/C catalysts. For the PtRu/C catalyst, CO is electrochemically oxidized at 0.28 V. In case of PtRu/SnO_2/C, CO is electrochemically oxidized at 0.13 V. This result indicated that SnO_2 addition improved activity for electrochemical CO oxidation. Maillaerd et al. reviewed the electrochemical CO oxidation on Pt-Ru[40]. Based on the bifunctional mechanism, CO is preferably adsorbed on Pt for Pt-Ru/C,

$CO + S(Pt\text{-}Ru) \rightarrow CO\text{-}S(Pt)$ (1)

S(Pt−Ru) is a surface site on the Pt−Ru alloy, while CO−S(Pt) is CO adsorbed on the Pt. H_2O is oxidized to form OH group preferably on Ru surface.

$H_2O + S(Pt\text{-}Ru) \rightleftarrows OH\text{-}S(Ru) + H^+ + e^-$ (2)

OH-S(Ru) is OH adsorbed on Ru. CO reacts with OH to form CO_2.

$CO\text{-}S(Pt) + OH\text{-}S(Ru) \rightarrow CO_2 + H^+ + e^- + 2S(Pt\text{-}Ru)$ (3)

For Pt-Ru/SnO_2/C catalyst, not only above reactions (2) and (3), but also following reactions (4) and (5) proceed

$H_2O + S(SnO_2) \rightleftarrows OH\text{-}S(SnO_2) + H^+ + e^-$ (4)

$CO\text{-}S(Pt) + OH\text{-}S(SnO_2) \rightarrow CO_2 + H^+ + e^- + S(Pt\text{-}Ru) + S(SnO_2)$ (5)

$S(SnO_2)$ is surface site of SnO_2, while $OH\text{-}S(SnO_2)$ is OH adsorbed on SnO_2. It is obvious that the Pt-Ru/SnO_2/C catalyst showed the lowest onset potential. By bifunctional mechanism, the enhancement of activity for electrochemical CO oxidation by the SnO_2 addition, was quantitatively evaluated by CO stripping voltammetry.

In situ IRRAS

By the FTIR results from our previous research showed that Pt/SnO_2, which has better CO oxidation, also has less CO tolerance than PtRu/C[41], the ranking of CO stripping and tolerance of the catalysts are as follow;

CO oxidation by CO stripping: Pt/SnO_2 > PtRu > Pt

CO tolerance by MEA analysis: PtRu > Pt/SnO_2 > Pt

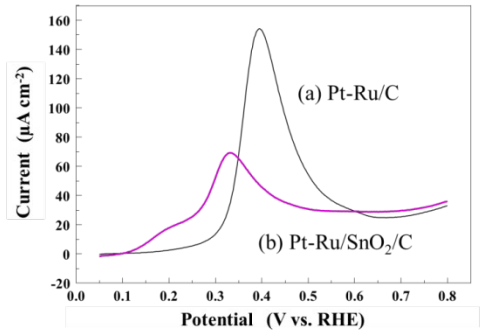

Fig. 4. CO stripping voltammetry at 60°C for (a) Pt-Ru/C and (b) Pt-Ru/SnO_2/C. CO was (1) fed for 20 min at 0.05 V in 0.1 M $HClO_4$; (2) purged for 30 min; and (3) swept at 60°C between 0.05 and 0.8 V at 10 mV/s.

In situ IRRAS measurement was carried out to observe CO_2 formation on the catalyst surface during the electrochemical CO oxidation. Fig. 5 shows in situ IR spectra obtained from the Pt-Ru/C and Pt-Ru/SnO_2/C surface in CO-dissolved 0.1 M $HClO_4$ solution, in the potential region between 0.0 and 0.6 V. As shown in Figure 5 (a), at 0.20 V, a new positive peak and a new negative peak appear at around 2340 cm^{-1} and 2030 cm^{-1}, which can be assigned to C-O stretching mode of CO_2 and Pt-adsorbed CO, respectively. Figure 5(a) and (b) shows integrated IR intensities of generated CO_2 and reacted CO for Pt-Ru/C and Pt-Ru/SnO_2/C catalyst. These figures indicate that CO is oxidized over 0.2 V on Pt-Ru/C, while CO is oxidized over 0.1 V on Pt-Ru/SnO_2/C. Rate of CO_2 formation Pt-Ru/SnO_2/C over 0.2 V is higher than that on Pt-Ru/C. Although CO oxidation peak cannot be observed by FTIR under 0.2 V, PtRu/C is well known as a high CO tolerance catalyst. Therefore, it can be considered that CO tolerance is not only depending on CO oxidation. The evaluation of bond strength is necessary to confirm the effect of adding SnO_2. Moreover, addition of metal oxide such as SnO_2 enhances electrochemical CO oxidation, but it might possibly reduce HOR activity.

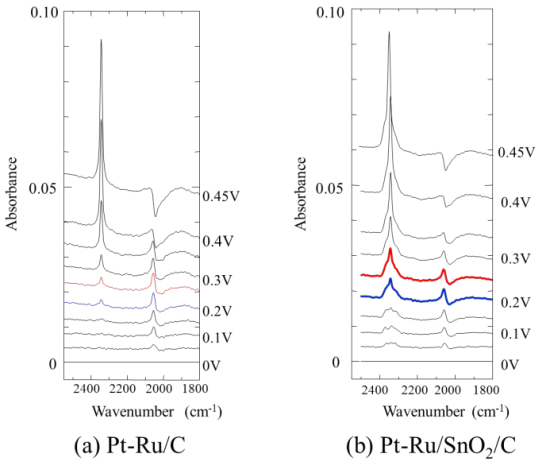

Fig. 5. IRRAS spectra of (a) Pt-Ru/C and (b) Pt-Ru/SnO_2/C deposited on a gold substrate surface CO was (1) fed for 20 min at 0.0 V in 0.1 M $HClO_4$; (2) purged for 35 min; (3) the electrode was pushed onto the CaF_2 prism window with the thin-layer geometry; the in situ IR spectra were recorded with a scan rate of 0.25 mV/s; 25 interferograms were co-added to each spectrum.

In situ SEIRAS

For the in situ SEIRAS measurements, CO was adsorbed at -150 mV, the potential was stepped to -200 mV and a series of spectra were taken at each potential in the range of -200 to 800 mV at 50 mV intervals. Fig. 6 shows the potential dependent FTIR spectra of CO adsorbed at saturation on Pt-Ru/C (Fig. 6(a)) and Pt-Ru/ SnO_2 /C (Fig. 6(b)) catalyst. The spectrum observed at 800 mV was used as a reference. Linear bonded CO at Pt sites were observed at 2009-2020 cm^{-1} for Pt-Ru/C and 2014-2025 cm^{-1} for Pt-Ru/SnO_2 /C.

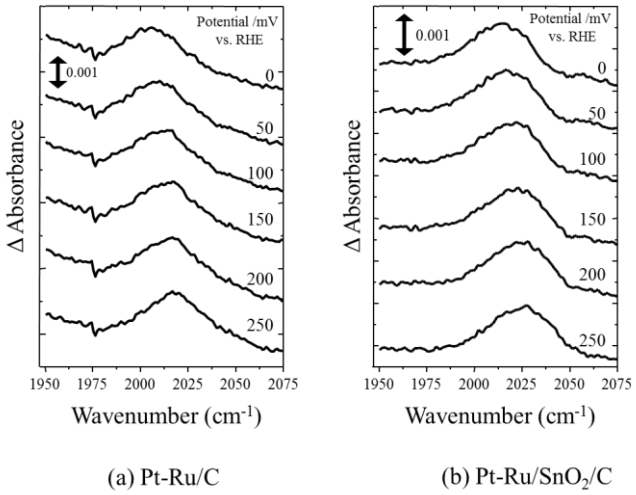

Fig. 6. SEIRAS spectra of adsorbed CO as a function of potential on (a) Pt-Ru/C and (b) Pt-Ru/SnO_2/C in 0.5 M H_2SO_4.

Potential dependence of the peak wavenumber is plotted in Fig. 7 for Pt-Ru/C and Pt-Ru/ SnO_2 /C catalyst. Linear frequency shift were observed for both Pt-Ru/C and Pt-Ru/SnO_2/C catalysts with dῡ/dE = 42 and 44 cm^{-1}/V, respectively in the potential region where CO adsorbed on the surface. This peak shift to higher wavenumber with increasing potential can be explained as a lowering of the metal-CO binding due to the decreasing of back-donation from metal to CO[42]. The wavenumber of CO stretching band adsorbed on Pt-Ru/SnO_2/C always appeared ca. 5 cm^{-1} higher than the CO stretching band adsorbed on Pt-Ru/C in the potential range between -200 mV to 50 mV. Since the coverage of CO decreases with an increase in the electrode potential, the peak wavenumber can shift by change of the dipole-dipole interactions as mentioned[43, 44]. Hoffman also reported that the peak could slightly shift to the higher wavenumber with an increase in CO coverage. In this potential range surface is fully covered with CO for Pt-Ru/C, but not fully covered with CO in case of Pt-Ru/SnO_2/C (as shown in Fig. 4). Thus, the peak shift to higher wavenumber observed in Pt-Ru/SnO_2/C even with a small amount of desorbed CO can be explained by lowering of the metal-CO binding which result in adsorbed CO to be easily oxidized on

Pt-Ru/SnO_2/C compared to Pt-Ru/C. Sato et al also report the weaken of Pt-CO bond strength by sublayer of Pt-Ru alloy[45] and particle size by similar technic[46]. The CO-Pt bond strength was quantitatively evaluated by in situ SEIRAS measurements. Ligand effect of SnO_2 on Pt-Ru catalyst was evaluated by this method. However, if addition of metal oxide reduces the HOR activity, ligand effect did not contribute to CO tolerance.

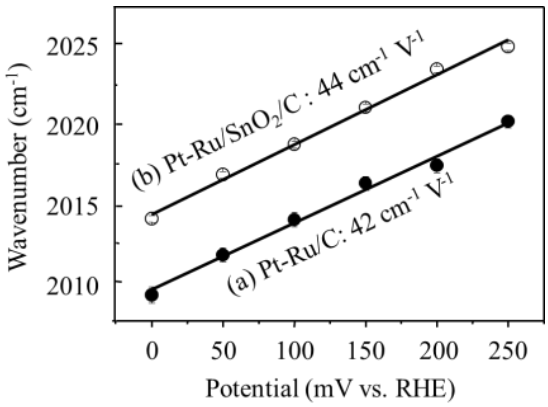

Fig. 7. The CO stretching peak frequency vs. potential for (a) Pt-Ru/C and (b) Pt-Ru/SnO_2/C.

CO tolerance

The effect of CO concentration on cell voltage at 0.2 A/cm^2 is shown in Fig. 8. Pt-Ru/C catalyst and Pt-Ru/SnO_2/C showed the same cell voltage as high as 0.78 V at 0.2 A/cm^2 in the absence of CO. This means that HOR activity of Pt-Ru/SnO_2/C is completely the same as Pt-Ru/C catalyst, as is suggested by XRD measurement and STEM observation. In our previous study SnO^{2-} modified Pt-Ru/C having high CO tolerance showed cell voltage of 0.76 V at 0.2 A/cm^2 in the absence of CO, which is 0.02 V lowers than that of Pt-Ru/C. While addition of SnO_2 reduce the HOR activity a little for SnO_2-modified Pt-Ru/C in the previous study, addition of SnO_2 does not reduce the HOR activity at all for Pt-Ru/SnO_2/C in the present study.

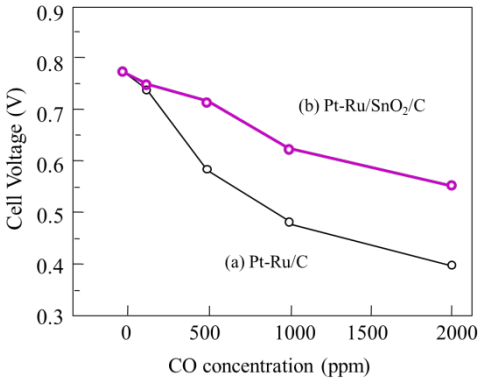

Fig. 8. Effect of CO concentration on cell voltage at 0.2 A/cm^2.

Cell temp.: 70°C; electrolyte: nafion NRE 212; cathode: Pt/C (0.5 mg/cm2); O_2 humidified at 70°C; flow rate: 80 mL/min; anode: (a) Pt-Ru/C and (b) Pt-Ru/SnO_2/C (0.5 mg Pt-Ru/cm^2); H_2 containing 0–2000 ppm CO humidified at 70°C; and flow rate: 80 mL/min.

Pt-Ru/SnO_2/C catalysts showed higher cell voltage than Pt-Ru/C catalyst in the presence of CO. Pt-Ru/SnO_2/C shows the cell over 0.7 V at 0.2 A/cm^2 in the presence of 500 ppm CO, and enhancement of CO tolerance is due to the SnO_2 addition.

Conclusions

Electrochemical CO oxidation, Pt-CO bond strength, and HOR activity in MEA were quantitatively evaluated by CO stripping voltammetry, SEIRAS, and fuel cell test. Addition of SnO_2 does not reduce the HOR activity at all for Pt-Ru/SnO_2/C. The weakening of Pt-CO bond strength contributes to CO tolerance, resulting in much higher activity in the presence of CO than commercial Pt-Ru/C catalyst.

Acknowledgements

This work was partly supported by the New Energy and Industrial Technology Development Organization (NEDO) Japan.

Notes and references

1. M. Watanabe and S. Motoo, *J Electroanal Chem*, 1975, **60**, 267-273.
2. M. Watanabe and S. Motoo, *J Electroanal Chem*, 1975, **60**, 275-283.
3. H. Igarashi, T. Fujino and M. Watanabe, *J Electroanal Chem*, 1995, **391**, 119-123.
4. H. A. Gasteiger, N. M. Markovic and P. N. Ross, *J Phys Chem-Us*, 1995, **99**, 8945-8949.
5. M. Watanabe, Y. M. Zhu and H. Uchida, *J Phys Chem B*, 2000, **104**, 1762-1768.
6. H. Igarashi, T. Fujino, Y. Zhu, H. Uchida and M. Watanabe, *Phys Chem Chem Phys*, 2001, **3**, 306-314.
7. X. Lu, Z. Deng, S. Wei, Q. Zhu, W. Wang, W. Guo and C.-M. L. Wu, *Catalysis Science & Technology*, 2015, **5**, 3246-3258.
8. S. Mukerjee, R. C. Urian, S. J. Lee, E. A. Ticianelli and J. McBreen, *Journal of the Electrochemical Society*, 2004, **151**, A1094-A1103.
9. J. Shim, C. R. Lee, H. K. Lee, J. S. Lee and E. J. Cairns, *Journal of Power Sources*, 2001, **102**, 172-177.
10. A. Ueda, Y. Yamada, T. Ioroi, N. Fujiwara, K. Yasuda, Y. Miyazaki and T. Kobayashi, *Catalysis Today*, 2003, **84**, 223-229.
11. T. Takeguchi, Y. Anzai, R. Kikuchi, K. Eguchi and W. Ueda, *Journal of the Electrochemical Society*, 2007, **154**, B1132-B1137.
12. T. Ioroi, K. Yasuda, Z. Siroma, N. Fujiwara and Y. Miyazaki, *Journal of the Electrochemical Society*, 2003, **150**, A1225-A1230.
13. M. T. M. Koper, T. E. Shubina and R. A. van Santen, *The Journal of Physical Chemistry B*, 2002, **106**, 686-692.
14. J. Nakamura, *Carbon*, 2015, **85**, 443-444.
15. E. Yoo, T. Okada, T. Kizuka and J. Nakamura, *Journal of Power Sources*, 2008, **180**, 221-226.

16. J. Oh, E. Yoo, C. Ono, T. Kizuka, T. Okada and J. Nakamura, *Journal of Power Sources*, 2008, **185**, 886-891.
17. T. Kondo, K.-i. Izumi, K. Watahiki, Y. Iwasaki, T. Suzuki and J. Nakamura, *The Journal of Physical Chemistry C*, 2008, **112**, 15607-15610.
18. A. E. Russell, S. Maniguet, R. J. Mathew, J. Yao, M. A. Roberts and D. Thompsett, *Journal of Power Sources*, 2001, **96**, 226-232.
19. B. N. Grgur, N. M. Markovic and P. N. Ross, *J Serb Chem Soc*, 2003, **68**, 191-205.
20. B. N. Grgur, N. M. Markovic and P. N. Ross, *The Journal of Physical Chemistry B*, 1998, **102**, 2494-2501.
21. G. X. Wang, T. Takeguchi, T. Yamanaka, E. N. Muhamad, M. Mastuda and W. Ueda, *Appl Catal B-Environ*, 2010, **98**, 86-93.
22. S. Axnanda, Z. Zhu, W. Zhou, B. Mao, R. Chang, S. Rani, E. Crumlin, G. Somorjai and Z. Liu, *The Journal of Physical Chemistry C*, 2014, **118**, 1935-1943.
23. N. Kamiuchi, T. Matsui, R. Kikuchi and K. Eguchi, *The Journal of Physical Chemistry C*, 2007, **111**, 16470-16476.
24. J. G. Zhou, H. T. Fang, J. M. Maley, J. Y. P. Ko, M. Murphy, Y. Chu, R. Sammynaiken and T. K. Sham, *The Journal of Physical Chemistry C*, 2009, **113**, 6114-6117.
25. N. M. Marković, B. N. Grgur, C. A. Lucas and P. N. Ross, *The Journal of Physical Chemistry B*, 1999, **103**, 487-495.
26. N. M. Marković, C. A. Lucas, B. N. Grgur and P. N. Ross, *The Journal of Physical Chemistry B*, 1999, **103**, 9616-9623.
27. L. Johnson, A. Ejigu, P. Licence and D. A. Walsh, *The Journal of Physical Chemistry C*, 2012, **116**, 18048-18056.
28. N. Narischat, T. Takeguchi, T. Tsuchiya, T. Mori, I. Ogino, S. R. Mukai and W. Ueda, *The Journal of Physical Chemistry C*, 2014, **118**, 23003-23010.
29. M. Wakisaka, S. Mitsui, Y. Hirose, K. Kawashima, H. Uchida and M. Watanabe, *The Journal of Physical Chemistry B*, 2006, **110**, 23489-23496.
30. T. Takeguchi, T. Yamanaka, K. Asakura, E. N. Muhamad, K. Uosaki and W. Ueda, *J Am Chem Soc*, 2012, **134**, 14508-14512.
31. T. Yamanaka, T. Takeguchi, G. X. Wang, E. N. Muhamad and W. Ueda, *Journal of Power Sources*, 2010, **195**, 6398-6404.
32. T. Wadayama, H. Yoshida, K. Ogawa, N. Todoroki and Y. Yamada, *Applied Surface Science*, 2010, **256**, 4517-4521.
33. C. Quijada, A. Rodes, F. Huerta and J. L. Vazquez, *Electrochimica Acta*, 1998, **44**, 1091-1096.
34. D. Chu, D. Gervasio, M. Razaq and E. B. Yeager, *J Appl Electrochem*, 1990, **20**, 157-162.
35. M. Osawa, K.-I. Ataka, M. Ikeda, H. Uchihara and R. Nanba, *Anal Sci*, 1991, **7**, 503-506.
36. S. Ye, T. Haba, Y. Sato, K. Shimazu and K. Uosaki, *Phys Chem Chem Phys*, 1999, **1**, 3653-3659.
37. H. Miyake, S. Ye and M. Osawa, *Electrochem Commun*, 2002, **4**, 973-977.
38. E. Antolini and F. Cardellini, *J Alloy Compd*, 2001, **315**, 118-122.
39. D. Wang, L. Zhuang and J. T. Lu, *J Phys Chem C*, 2007, **111**, 16416-16422.
40. F. Maillard, G. Q. Lu, A. Wieckowski and U. Stimming, *J Phys Chem B*, 2005, **109**, 16230-16243.
41. T. Takeguchi, Y. Anzai, R. Kikuchi, K. Eguchi and W. Ueda, *Journal of The Electrochemical Society*, 2007, **154**, B1132-B1137.
42. S. C. Chang and M. J. Weaver, *Surface Science*, 1990, **238**, 142-162.
43. S. C. Chang and M. J. Weaver, *The Journal of Chemical Physics*, 1990, **92**, 4582-4594.
44. F. M. Hoffmann, *Surface Science Reports*, 1983, **3**, 107-192.
45. T. Sato, K. Kunimatsu, K. Okaya, H. Yano, M. Watanabe and H. Uchida, *Energy & Environmental Science*, 2011, **4**, 433-438.
46. T. Sato, K. Okaya, K. Kunimatsu, H. Yano, M. Watanabe and H. Uchida, *ACS Catalysis*, 2012, **2**, 450-455.